University of Nairobi

Institute of Nuclear Science and Technology

Pre-Mining Concentrations Of Heavy Metal Elements and Radioactivity Concentrations Of Primordial Radionuclides in Soils Around the Niobium Mining Site in Kwale County, Kenya

by

Maiyo K. Benson

S56/74422/2012

A thesis submitted in partial fulfilment for the degree of Master of Science in Nuclear Science in the Institute of Nuclear Science and Technology, University of Nairobi.

Declaration

This thesis is my original work and has not been submitted in support of award of any degree or qualification in any other University.

Signature …….. Date ……

Maiyo K. Benson - S56/74422/2012

Supervisors' approval

This thesis has been submitted for examination with our knowledge as University Supervisor(s)

Prof. Michael J. Gatari Signature……

Institute of Nuclear Science &Technology Date……

P.O. Box 30197- 00100, Nairobi

Mr. Michael Mangala Signature ……..…….

Institute of Nuclear Science &Technology Date ……

P.O. Box 30197- 00100, Nairobi

Dedication

I dedicate this research work to my family members for their support during my study period.

Acknowledgement

I am so grateful to the Almighty God for the protection and good health throughout the entire study period.

I would also like to thank my supervisors, Dr. Michael J. Gatari, the late Mr. David M. Maina and Mr. Michael Mangala for providing me with the necessary guidance and support. I am especially indebted to them for their patience and encouragement when I encountered some delays in the course of the project.

I would like to acknowledge the staff at the Institute of Nuclear Science and Technology for their support and help during my lab work.

I am grateful to Kenya Nuclear Electricity Board (KNEB) for their generosity of sponsoring my studies at the Institute of Nuclear science and Technology and also to National Council for Science and Technology for funding my research.

Above all, I wish to thank my fellow students and anyone who might have played a role towards the success of this project.

Abstract

An elemental analyses and radiological survey of soils around proposed Nb and rare earth mining site in Mrima Hill, Coastal Kenya, was conducted with an aim of providing the status of elemental and radionuclides concentrations. Elemental analysis was done using EDXRF spectroscopy, while HPGe gamma spectroscopy was used for determination of the activity. Most elements were determined at concentration levels above the recommended limits in agricultural soils. For instance, Fe, Mn and Ti were found to be the major constituent in the soil samples with mean concentration of 29%, 7.5% and 3.4% respectively. Other soil constituents include Zn (94 - 2549 μg g^{-1}), Pb (205 – 2661 μg g^{-1}) and Sr (551 – 6606 μg g^{-1}). Concentrations higher than the normal range of 10 - 20 μg g^{-1} in soils were reported for Nb, at a range of 151 – 7511 μg g^{-1}. Similar observations were made with respect to rare earth elements i.e. Y (100 – 2776 μg g^{-1}) and Zr (142 – 542 μg g^{-1}). These values can be associated with the huge mineral deposits, particularly Nb and rare earths, discovered in the region. These results are however comparable to a previous study conducted in the area. Activity levels above global average were recorded for ^{232}Th and ^{238}U, with mean concentrations of 1400 ± 795 Bq kg^{-1} for ^{232}Th and 143 ± 11 Bq kg^{-1} for ^{238}U. However, ^{40}K was determined at levels below global average, with a mean of 200 ± 92 Bq kg^{-1}. Using these measured activity and conversion factors, radiological risks were assessed. Radiation hazard indices that include; radium equivalent dose, representative gamma index, annual effective dose, external hazard index and absorbed dose rate were calculated. All the indices were found above the recommended limits. Therefore, Mrima Hill can be confirmed as a high background radiation area.

Table of Contents

Declaration i

Dedication ii

Abstract iv

List Of Tables vii

List Of Figures viii

Chapter One 1

Introduction 1

1.1 Background 1

1.2 Problem Statement 3

1.3 Justification and significance of the research project 4

1.3 Objectives of the study 4

1.5 Scope 5

Chapter Two 6

Literature Review 6

2.1 Naturally Occurring Radioactivity 6

2.2 Natural Radioactivity measurements 8

2.3 Effects of Ionizing Radiation on Health 12

2.4 Heavy Metal Concentrations in Mining Areas 13

Chapter Three 15

Methodology 15

3.0 Introduction 15

3.1 Description of the Study Area 15

3.2 Sampling 15

3.3 Sample Preparation 17

3.3.1 EDXRF Samples 17
3.3.2 Gamma Spectroscopy samples 17
3.4 Sample Analyses 17
3.4.1 Gamma-ray Spectrometry Analysis 17
3.4.2 EDXRF Analysis 21
3.5 Data Analyses 22
3.5.1 Potential Radiological Hazards Assessment 22
3.5.2 Absorbed dose rate and annual effective dose determination 23
Chapter Four 24
Results And Discusion 24
4.0 Introduction 24
4.1 Quality Assurance 24
4.1.1 Accuracy of EDXRF Spectroscopy Method 24
4.1.2: Accuracy of Gamma Spectroscopy 26
4.2 Elemental Concentration 27
4.2.1 Heavy Metals 27
4.2.2 Rare Earth Elements 32
4.2.3 Radionuclides 32
4.3 Activity 34
4.4 Evaluation of Radiological Hazards 41
Chapter Five 46
Conclusions And Recommendations 46
5.1 Conclusions 46
5.2 Recommendations 47
References 48

List Of Tables

Table 2.1 Annual per capita effective doses in year 2000 from natural and man-made sources

Table 2.2: Average radiation dose from natural sources

Table 3.2: Recommended energy lines for gamma-ray analysis of environmental samples

Table 4.1: Results of the analyses of PTXRF-IAEA-09 river clay

Table 4.2: Detection limits of various elements using EDXRF spectroscopy

Table 4.3: Results of analyses of RG-K, RG-Th and RG-U standard reference material

Table 4.4: Results of analyses of IAEA-375 certified reference material

Table 4.5: Elemental concentrations in soil samples

Table 4.6: Concentration levels of Y, Nb, Ce, Th and U

Table 4.7: Activity concentration of ^{232}Th, ^{238}U and ^{40}K in $Bqkg^{-1}$

Table 4.8: Estimated values for radium equivalent dose, external hazard index, representative gamma index, absorbed dose rateand annual effective dose

List Of Figures

Figure 2.1: Uranium decay series

Figure 2.2: Thorium Decay series

Figure 3.1: Google map of the proposed niobium mining site in Mrima Hill, Kwale County

Figure 3.2: Map showing sampling points at Mrima Hill.

Figure 3.3: A set up of HPGe gamma spectroscopy

Figure 4.1: Trends and distribution patterns of ^{232}Th, ^{238}U and ^{40}K

Figure 4.2 Correlation analyses between elemental concentration and activity concentration levels for potassium

Figure 4.3: Correlation analyses between elemental concentration and activity concentration levels for uranium

Figure 4.4: Correlation analyses between elemental concentration and activity concentration levels for Thorium

Figure 4.5: A graph showing how activity concentration of uranium correlates with those of potassium in the sampled area

Figure 4.6: A graph showing how activity concentration of uranium correlates with those of thorium in the sampled area

Figure 4.7: A graph showing how activity concentration of potassium correlates with those of thorium in the sampled area.

Chapter One

Introduction

1.1 Background

Human beings are constantly exposed to ionizing radiation emanating from artificial and natural sources. The natural radiation sources include cosmic rays and NORMs contained in soil, air, water and plants, accounting for over 80% of received radiation dose (Nisar et al., 2015). In soils, majority of NORMS are radionuclides from the thorium series (^{232}Th), uranium series (^{238}U), ^{40}K and the radioactive gas radon (Nisar et al., 2015; Ademola et al., 2014; Sanchez-Gonzarez et al., 2014). This lead to internal and external radiological hazards as a result of the emitted gamma rays and inhalation of radon and its daughters. On the other hand, manmade exposures are mainly from nuclear reactors, X-ray and other radiation generators used for medical, industrial, among other activities.

Natural radioactivity depends largely on the geographical and geological factors (UNSCEAR, 2000). The radioactivity level resulting from these NORMs is referred to as background radiation that depends on the concentration of the radio nuclides in the environment. It is usually high in locations having mineral deposit such as uranium ores, carbonates and phosphates (Oyedele, 2006), and in situation where the environment is polluted from either natural or anthropogenic activities. For instance, mineral deposits could find their way to the soil surface via processes like mining, weathering processes. Furthermore, leaching of these radionuclides into groundwater system, can lead to widespread contamination.

Heavy metal pollution is of particular concern due to the toxicity, persistence and bio-accumulative properties of the metals. These metals occur both in natural and contaminated environments, and in general, lower concentrations are observed in natural environment. However, anthropogenic activities such as exploration and mining have led to increased concentration of these metals in the environment, since their rates of generation are more rapid relative to natural processes. Some of the heavy metals play a significant role in nature. For example, Cu, Co, Zn, Mo, Mn and Fe are required as catalyst for enzymatic activities (Adepoju-Bello and Alabi, 2009). Exposure to these essential metals in high concentrations can however be toxic. Others such as lead, cadmium and mercury, have no known physiological role (Akan et al., 2010).

The mineral potential of sedimentary rocks in the Kenyan includes; silica sands at Waa, Ramisi and Msambweni; titanium (zircon, ilmenite, rutile) at Shimba Hills and Nguluku; Rare Earth Elements (phosphates, niobium) at Mrima Hills; Gemstones at Kuranze; copper, lead and zinc at Mwache, Mkang'ombe, Dzitenge and Dumbule; Coal at Maji ya Chumvi; sandstones at Mariakani; and Baryte at Lunga-lunga (KCG, 2015). Although exploration of these minerals at full potential will be of great economic value, it however comes at a cost. For instance, mining activities usually lead to elevated elemental concentrations in the environs (Karangwa, 2012), leading to contamination of soil, water and eventually food crops. Mining also leads to increase in relative concentration of the Norms (Patel, 1991).

According to UNSCEAR (2000), the great interest expressed worldwide for the study of NORMs and radioactivity have led to the extensive surveys to be undertaken in many countries of the world. Kenyan coastal region in particular, has been of great interest for research since it is believed to have high background radiation. In particular, studies conducted in Mrima Hill indicated that a certain amount of radioactive matter may be present within the mined materials. According to RPB (1999), some patterns of high radioactivity were reported in some areas of the South Coast area, confirming the results of Patel (1991), where high gamma radiation levels at and around Mrima hill area were reported. The board further carried out external radiation measurements along the roads known to have been graveled using materials from the area. Roads in Mombasa Island were also surveyed for comparison as a

control area. Radiation levels from roads in Mombasa Island were found to be relatively lower; about 90 Bq kg^{-1} of ^{232}Th on average, as compared to roads where gravel from Mrima Hill was used, with activity levels as high as 1200 Bq kg^{-1} being recorded.

In 2013, there have been increased anthropogenic activities around Mrima Hill. Prospective studies had been concluded and mining of Nb and rare earths was set to commence. In order therefore to copnstrain the impact of mining activities in the future, it necessitates a pre-operational baseline study to be conducted. Soil samples from the site were collected and analyzed for elemental content as well as assessment of radiological risks using XRF and gamma spectroscopy respectively. This helps to assess both radiological and non-radiological risks

1.2 Statement of the Problem

Huge deposits of Nb and rare earths have been discovered in Mrima hill, with exploration activities set to commence. Although environmental impact assessment study has been undertaken by the Kenyan government and the project given a green light, exposure to the naturally occurring radioactive materials (NORMs) is usually enhanced through mining/excavation works and processing of minerals. According to UNSCEAR report (2000), communities living near mining operations may be exposed to about 100 times the normal background levels (2.4 mSv y^{-1}). In Addition, metal concentration levels in and around the mining areas are similarly elevated.

According to UNSCEAR (1993), information on exposures of members of the public resulting from the mining activities is extremely scarce. This calls for elemental and radiological monitory studies to be regularly conducted. It is in this understanding that this project was conducted. This project is therefore intended to provide baseline values of the radioactivity and heavy metal concentration levels in soil around the proposed Nb and rare earth mines. The study will also assess any changes in these levels, comparative to the past studies.

1.3 Justification and significance of the research project

Mrima Hill has been classified as a high radiation background area. However, the last studies in the area were conducted over two decades ago. In particular, Patel and Mangala (1994) associated these high levels with occurrence of thorium and uranium, while Patel (1991) associated the observation with presence of carbonatite rocks. Therefore, in order to understand if there are any changes with respect to radiological levels and elemental concentrations, this study is essential.

This study endeavors to determine the specific radiation levels around the proposed mining site, as well as elemental concentration. The study is therefore expected to create awareness to miners, the local population, and regulatory bodies on hazards posed, and in designing radiation protection control guidelines if necessary. Additionally, the results obtained in this study, together with data from other studies done earlier, will enable projections on the possible levels of radioactivity and elemental concentrations enhancement as a result of the mining activities.

1.3 Objectives of the study

Main objective

The study sort to analyse the elemental and radionuclides concentrations in soils around the Nb and rare earth mining project area in Mrima Hill, Kwale County.

Specific objectives

The Specific objectives are:

1. To determine heavy metal content in the soil samples.
2. To determine the concentration levels of Nb and rare earths in the soil samples.
3. To determine the activity of natural radionuclides; ^{40}K, ^{232}Th and ^{238}U in the soils around Mrima Hill and the potential radiological hazards posed by these radionuclides.

1.5 Scope

This study was conducted in Mrima Hill, Kwale County. The study focused on assessing the radiological hazards posed by NORMs, as well as determining elemental content. However, only topsoil samples were analysed (0 – 30 cm).

Chapter Two

Literature Review

2.1 Naturally Occurring Radioactivity

Most minerals have radionuclides of terrestrial origin, usually known as primordial radionuclides. The ^{232}Th decay series, ^{238}U decay series, and ^{40}K are the principal radionuclides (Ademola et al., 2014). The activity of these radionuclides in soils and rocks vary widely, but are usually low. However, certain minerals may contain thorium and uranium radionuclides at higher concentrations. Through industrial, physical, chemical and thermal processes, the natural equilibrium of the radionuclides can be disturbed causing an enhancement or decrease of certain radionuclides in comparison to the original matrix.

The parent radionuclide in uranium series is ^{238}U, which undergoes α decay with half-life of about $4.47 * 10^9$ years. The stable product in this series is ^{206}Pb and is reached after 8α and 6β decays (Figure 2.1). The common form of natural radiation in this series is radon gas (^{222}Rn), which is commonly found in soils and rocks. On the other hand, thorium series begin with ^{232}Th radionuclide, and has 100 % abundance. It undergoes decay with half-life of $1.41*10^9$ years. The series ends with a stable nuclide ^{208}Pb and is reached after 6α and 5β decays (Figure 2.2).

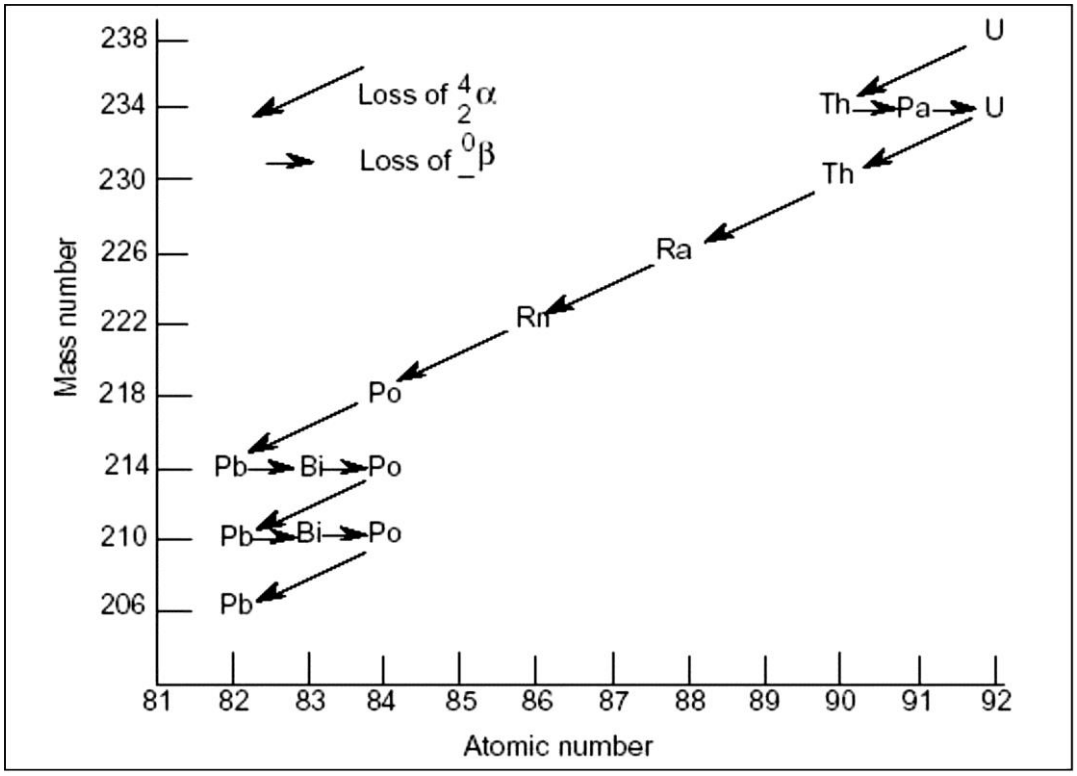

Figure 2-1: Uranium decay series (Adapted from Chang, 2005)

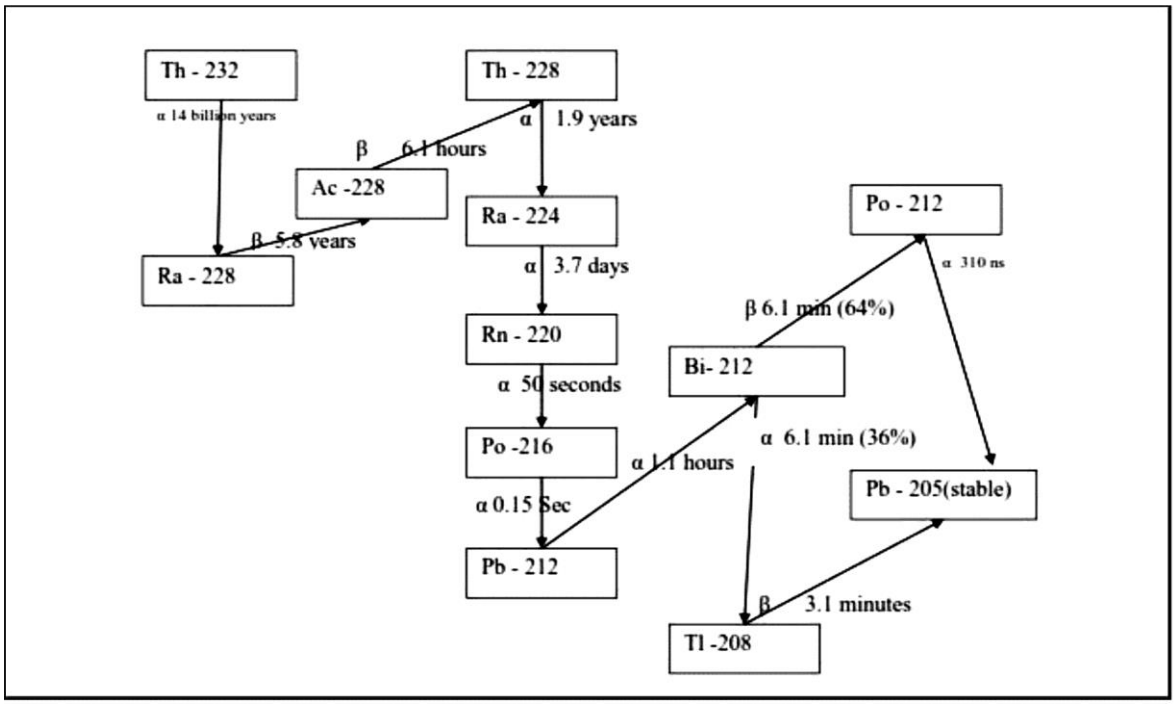

Figure 2.2: Thorium Decay series (ANL, 2005).

^{40}K is a major source of terrestrial radioactivity and accounts for 0.012% of natural potassium. It has a long half-life of1.25*10^{9} years, and decays mostly through β-

emission to ^{40}Ca. It is usually found within clay minerals and in many foodstuffs. Human being requires potassium to sustain various biological processes, where most of it (including ^{40}K) is almost entirely absorbed from gastrointestinal tract into the bloodstream upon ingestion (UNSCEAR, 2000). The ^{40}K that enters the bloodstream after inhalation or ingestion can easily be distributed to all organs and tissues. Through the emitted ionizing radiation it can cause cancer.

2.2 Natural Radioactivity measurements

Sources of radiation exposures can be classified into four main categories; natural radiation exposures, man-made environmental exposures such as nuclear weapon test, medical radiation exposures resulting from use of ionizing radiation for therapy and medical diagnosis, and occupational exposures. Table 2.1 gives a summary of some of these sources for year 2000 and their effective dose and trends (UNSCEAR, 2000). Natural exposures result from presence of NORMs within the earth's crust and cosmic rays (Table 2.2), which is a topic of interest in this study.

Table 2.1 Annual per capita effective doses in year 2000 from natural and man-made sources (UNSCEAR 2000)

Source	Worldwide annual per caput effective dose (mSv)	Range or trend in exposure
Natural background	2.4	Typically ranges from 1-10 mSv, depending on circumstances at particular locations, with sizeable population also at 10-20 mSv.
Diagnostic medical examinations	0.4	Ranges from 0.04-1.0 mSv at lowest and highest levels of health care Has decreased from a maximum of 0.15 mSv in 1963. Higher in northern hemisphere and lower in southern hemisphere
Atmospheric nuclear testing	0.005	Has decreased from a maximum of 0.04 mSv in 1986 (average in northern hemisphere). Higher at locations nearer accident site
Chernobyl accident	0.002	Has increased with expansion of program but decreased with improved practice
Nuclear power production	0.0002	

Table 2.2: Average radiation dose from natural sources (UNSCEAR, 2000)

Source effective dose (mSv)	Worldwide average annual (mSv)	Typical range (mSv)
External exposure		
Cosmic rays	0.4	0.3 - 1.0
Terrestrial gamma rays	0.5	0.3 - 0.6
Internal exposure		
Inhalation (mainly radon)	1.2	0.2 - 10
Ingestion	0.3	0.2 - 0.8
Total	2.4	1 - 10

Radiation exposures resulting from the extraction and processing of minerals is an issue of concern. On average, the annual effective dose worldwide arising from the extraction and processing of earth minerals, according to UNSCEAR (1993), is estimated to be about 20 mSv y^{-1}. This has lead to increase in number of radiological studies being conducted globally within the mines, suspected high background radiation areas, as well as recreational and residential areas such as beaches (Ademola, 2015; Sivakumara et al., 2014; Darko et al., 2005; Mustapha et. al., 2007). From such studies, there has been enhanced understanding of radiological hazards posed, leading to increased awareness. In addition, high background radiation areas have been mapped out. Such areas include Mrima Hill in Kenya (Patel 1991), Guarapari in Brazil (Paschoa, 2000), Yangjiang in China, which has been designated as controlled area (UNSCEAR, 2000; Wei et al., 1993), among others.

According to Mustapha et al. (1997), the average annual effective dose in Kenya is above the global average. In the study, the contributions of various sources to the total effective dose were determined as follows; 0.1 - 2.1 mSv y^{-1} from terrestrial gamma radiation; 0.22 - 0.75 mSv y^{-1} and a per capita of 0.5 mSv y^{-1} from cosmic radiation; and 0.5 to 6.1 mSv y^{-1} from inhalation of radon (^{222}Rn). In addition, Ingestion of

volcanic ash was identified as an internal exposure pathway, especially to pregnant women.

Use of construction materials from high background areas could result in widespread human exposures. Patel (1991), noted that roads constructed using gravel from Mrima Hill recorded high dose rates. Similar observations were made by Maina et al. (2002), where indoor radon levels in African cultural (mud) houses were investigated. More than half of the houses in Taita Taveta County were found to exceeded the 400 Bq m^{-3} limit (UNSCEAR 1993), as compared to houses in Rift valley where levels below 200 Bq m^{-3} were recorded. The author further computed the annual effective dose for the two regions, obtaining a range of 3.1 – 3.6 mSv y^{-1} in Taita Taveta region, and 0.4 – 2.6 mSv y^{-1} in Rift Valley.

Achola et al. (2012), conducted radioactivity and elemental analysis of carbonatite rocks from parts of western Kenya. The annual external effective dose rates in the area were found to be 5.7 mSv y^{-1}, approximately twelve times the global average of 0.46m Sv y^{-1}. The activity concentrations ranged from 14- 6560 Bq kg^{-1} with an average of 1396 Bq kg^{-1} for ^{232}Th; from 2 to 499 Bq kg^{-1} with an average of 179 Bq kg^{-1} for ^{238}U equivalent; and from 56 to 1454 Bq kg^{-1} with an average of 509 Bq kg^{-1} for ^{40}K. The author further found the absorbed dose rates in air outdoors at 1 m above the ground in the range of 700 - 6000 nGy h^{-1}, with an overall mean value of 2325 nGy h^{-1}. Therefore, this area was described as a high background radiation area. The findings concurred with Patel (1991), where carbonatite rocks were associated with presence of natural radionuclides and high background radiation.

Activity levels much higher than the global mean of 25 Bq kg^{-1} were obtained by Maina (2008) in Kwale, Coastal Kenya. On average, levels as high as 178 Bq kg^{-1} and 162 Bq kg^{-1} were recorded for ^{232}Th and ^{238}U respectively. However, contribution of ^{40}K was found to be negligible. The author further found a significant correlation between elemental concentrations of Ti, Fe, Zr and Nb with the activity concentration levels of radionuclides in the ^{232}Th and ^{238}U series. Using an occupancy factor of 0.2, the author estimated the annual effective dose to an adult at 1 m above the ground to be 156 μSv, which exceeds the world average effective dose (<70 μSv).

Darko et al. (2005), conducted a comparative study on occupational exposure to radiations, between underground and surface miners in Ashanti gold mines of Ghana. The underground miners were found to be more exposed with an average effective annual dose of 0.56 mSv y^{-1}, as compared to 0.11 mSv y^{-1} for surface miners. The authors attributed the higher dose rates in underground mines to radon gas. Radon is a product of ^{238}U decay series and is commonly trapped in rocks and soils. According to the author, this gas could easily find its way into air and water in the mines through diffusion and/or with gases like CO_2 and CH_4 or water moving in the soil horizons. This assertion was supported by Lipsztein et al. (2001), whereby radon gas was found to be key source of occupational exposure to coal miners in Brazil.

Foodstuff can also be a pathway through which human beings can be exposed to radiation through ingestion. Maina (2008) in a study on concentrations of radionuclides in selected foodstuffs and consumer products in Nairobi identified ^{40}K as the major contributor to annual ingestion dose as a result of food consumption ranging from 0.02 mSv y^{-1} for tea leaves to 0.16 mSv y^{-1} for maize meal. Infant milk was found to contribute 0.05 mSv y^{-1} on average.

2.3 Effects of Ionizing Radiation on Health

Radiation damage to tissue and organs depends on the absorbed dose, the type of radiation and the sensitivity of different tissues and organs. In order to understand the effect of radiation, extensive research is still being conducted to give information on the relationship between radiation exposure and specific health effects, both in the short and long term (UNSCEAR, 2012). These radiation effects can be classified as Deterministic effects i.e. those health effects that are caused by extensive cell death and/or cell malfunctioning, and stochastic effects initiated by the modification of the genetic material of only one or perhaps a few cells in a way that is still compatible with cell survival e.g. cancers, leukemia, and heritable diseases (UNSCEAR, 2012).

According to international commission on radiological protection ICRP (2007), deterministic effects mainly occur in the dose range above 100 mGy i.e. tissues express clinically relevant functional impairment. These effects become more severe as the dose rate increases, with even a possibility of death. Other effects include burns and

radiation sickness such as weakness, nausea, skin burns, hair loss and diminished organ function (EPA, 2012).

Stochastic effects include cancers and hereditary disorders, associated with long term, low level (<100 mSv) radiation exposure. The occurrence of these effects rise in direct proportion to increase in the equivalent dose, in the relevant tissues and organs (ICRP, 2007). A study by Preston et al. (2003), on mortality of atomic bomb survivors also associated stroke, heart disease, respiratory diseases and digestive disorders to low level radiation exposure.

2.4 Heavy Metal Concentrations in Mining Areas

Mining activities usually lead to land degradation and pollution. This leads to loss of beauty, as well as destruction of flora and fauna. However, elevated elemental concentrations, especially heavy metals have been a major concern in mining areas and environs. These metals are of special interest since they have a tendency to accumulate and persist in the environment for a very long period, due to their non- biodegradable nature. In addition, heavy metals have a tendency to bio-accumulate in living organism.

Odumo et al. (2011), carried out an assessment of major elements and their concentration in gold mining activities at Migori, southwestern Nyanza, Kenya. The concentrations in soil were determined in the range of: Ti (711 – 13,000 µg g^{-1}); Co (83 - 1,010 µg g^{-1}); Zn (30 – 63,210 µg g^{-1}); Au (14 – 73 µg g^{-1}); Cu (40 -118,533 µg g^{-1}) and Hg (16 – 150 µg g^{-1}). Pb and As were also determined in high quantities. The major elements and their concentrations in the water samples on the other hand were Cu (29 - 14,976 µg l^{-1} and Zn (34 - 683 µg l^{-1}). As, Pb and Zn were also detected in higher quantities, with average levels of 3274 µg g^{-1}, 1473 µg g^{-1} and 587 µg g^{-1}, respectively.

Karangwa (2012), evaluated the impact of tungsten mining on agricultural soils in Rwanda. Major constituents of soil were found to be Fe, Mn, Ti and Zr, with heavy toxic metals associated to tungsten mining, such as W, As and Pb in traces. The author attributed presence of tungsten and tailings in soils to poor extraction processing

methods used by the miners. Arsenic was determined at levels above the interventional value (50 μg g^{-1}).

An elemental analysis of carbonatite rock samples from Mrima Hill, Kenya, by energy dispersive X-ray fluorescence (EDXRF) was conducted by Patel and Mangala (1994). The concentration of rare earth elements such as Ce, Ba and Nb were found to be significant and worth exploitation, an assertion that has been confirmed by prospective studies conducted in the past. In addition, high heavy metal concentration levels were recorded. For instance, concentration ranges of Fe, Ti and Mn were determined at (5 – 30%), (0.3 – 17%) and (1.1 – 9%) respectively. On the other hand, ^{232}Th was identified as the main source of high environmental radiation in the area, with a mean concentration of 770 μg g^{-1}.

Maina (2008), carried out an assessment on heavy metal concentration levels in soils around titanium mining site in Kwale, coastal Kenya. The author identified Fe and Ti as the major elemental constituents, at 1.2% and 1.5% respectively. In determining the elemental concentration distribution patterns, the author revealed a significant correlation between concentration levels of Ti, Nb, Zr and Fe, with the activity concentration levels of radionuclides in the ^{232}Th and ^{238}U series. In a similar study, Ntihabose (2010) conducted an assessment of heavy metal fluxes due to extraction and processing of coltan ores in selected areas of Rwanda. Three categories of samples were assessed; processed coltan, extracted (or unprocessed) coltan, mine sediments and control soil samples. The highest concentration of Ta (30%), Nb (25%) and Sn (16%) were observed in processed Coltan. In some sediment samples Ta (35- 63 μg g^{-1}) and Nb (35-83 g g^{-1}) were also reported but at lower level. Heavy toxic elements such as Pb, Mn and Zn were also observed in all samples with Mn having the highest concentration at 35,155 - 65, 200 μg g^{-l}, and Pb with the lowest concentration at 548 - 1655 μg g^{-l}.

Chapter Three

Methodology

3.0 Introduction

This chapter describes the study area, sampling procedures, sample preparation, as well as the analytical methods used in determining elemental content and radioactivity levels in the collected samples. Methods for analyses of the obtained data are also discussed.

3.1 Description of the Study Area

The study area is located in the prospected Nb and rare earth mining site, in Mrima Hill. Mrima Hill (4.47801°S; 39.26116°E), is situated in Msambweni Constituency, Kwale County in the coastal plains of Kenya, approximately 65km southwest of Mombasa (Figure 3.1).

Mrima Hill, in Kwale County is among the top five regions in the world with rare earth deposits, with a potential in-ground value of up to Sh5.4 trillion (KCG, 2015).

3.2 Sampling

A total of forty sampling sites were randomly identified for soil sampling. Soil samples were collected at a depth of up to 30 cm. For each sampling sites, three different samples were obtained within a radius of 1 m. The three subsamples were homogenized to obtain a representative sample of about 0.5 kg and kept in well labeled polythene bags ready for transportation to the laboratory. The locations of the sampling sites were recorded using a Garmin eTrex 10 GPS. The recorded locations were used to generate a map of the sampling sites using a GPS software (Figure 3.2).

Fig. 3.1 Google map of the proposed Nb mining site in Mrima Hill, Kwale County

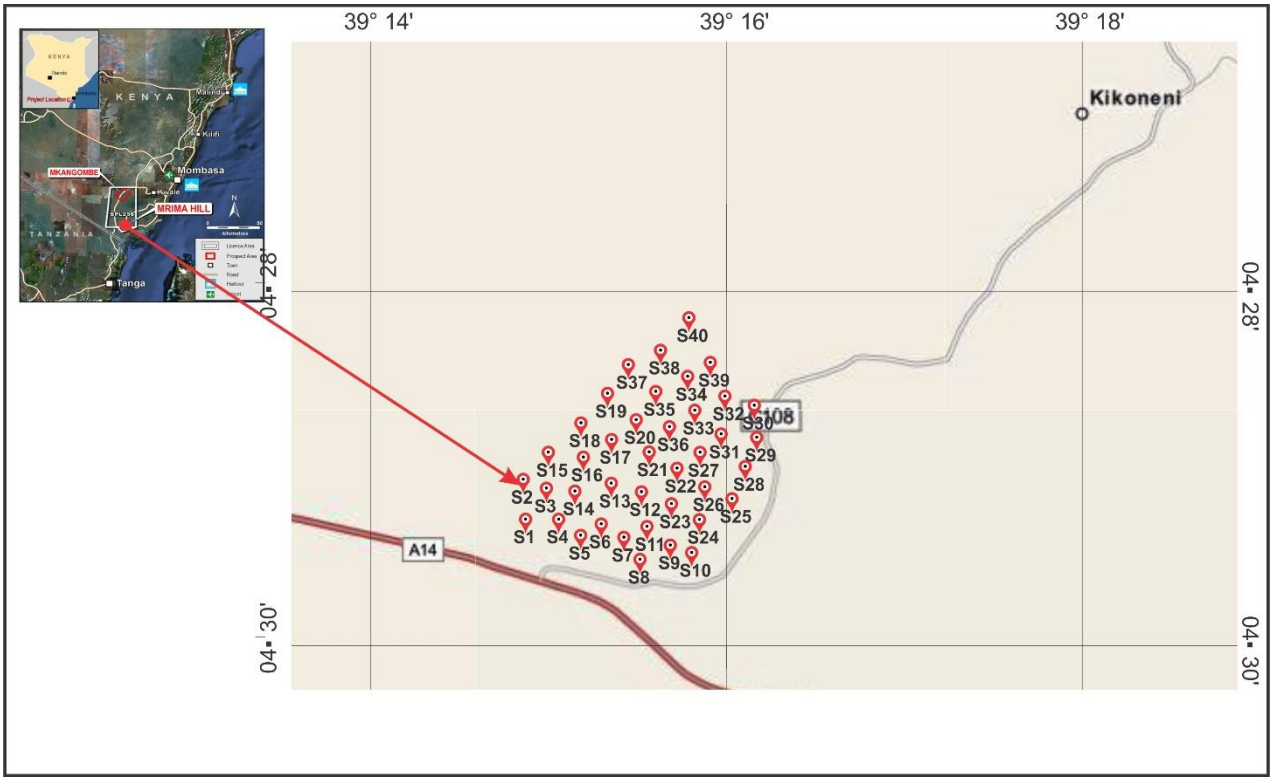

Fig. 3.2 Map showing sampling sites at Mrima Hill, generated by GPS software from stored locations in Garmin eTrex 10 GPS.

3.3 Sample Preparation

In the laboratory, the samples were first air dried for two weeks. To further reduce the moisture content, the samples were dried in an oven for a period of eight hours at 60 ^{o}c.The samples were then ground to break down aggregates. Grinding helps not only in size reduction, but also in ensuring homogeneity of the elements in the sample.

3.3.1 EDXRF Samples

For EDXRF, the samples were further crushed and pulverized into fine powder. The pulverized sample was then sieved to grain sizes $\leq$60 μm. About 1.4 g of the fine sample was mixed to homogeneity with about 0.4 g of cellulose i.e. 20% dilution. Three pellets, each weighing approximately 350 mg were prepared using a hydraulic press from each sample ready for EDXRF analysis. The pellets were labeled appropriately and kept in a petri dish to avoid contamination. This procedure was also used in preparation of the standard reference material.

3.3.2 Gamma Spectroscopy samples

About 300 g of the pulverized samples were sealed in 250 ml plastic containers for a period of one month prior to gamma analyses. This is to allow gaseous radon (half-life 3.8 days) and its short lived decay daughters (^{214}Bi and ^{214}Pb) to reach equilibrium with the long lived ^{226}Ra precursor in the sample.

3.4 Sample Analyses

Elemental analyses of the samples was done using EDXRF (Shimanzu EDX- 800HS model), whereas radioactivity measurements used high-purity germanium (HPGe) gamma-ray detector. Below is a brief discussion of the two analytical methods.

3.4.1 Gamma-ray Spectrometry Analysis

Activity of the NORMs in pulverized soil samples was performed with HPGe detector (Figure 3.3). Each sample was analysed for 12 hours. Prior to the sample measurement, the environmental gamma background radiation was assessed using an empty container. The background measurements were later deducted from the measured gamma-ray spectra of each sample to correct the net peak areas for the counts.

Figure 3.3: A set up of HPGe gamma spectroscopy at the Institute of Nuclear Science & technology

Based on the measured gamma-ray photo-peaks emitted by specific radio-nuclides in the ^{232}Th series, ^{238}U series, and in ^{40}K series, their activity in the samples were determined. These relied on the establishment of secular equilibrium in the samples due to the much smaller lifetime of daughter nuclides in the decay series of ^{232}Th and ^{226}Ra. More specifically, the ^{232}Th activity was determined from the average activity of ^{212}Pb and ^{228}Ac in the samples, while that of ^{238}U equivalent was determined from the average activity of the ^{214}Pb and ^{214}Bi decay products (Mohanty *et al*., 2004).

Calibration of the HPGe system is essential in acquiring accurate results (Gilmore & Hemingway, 1995). This ensures that the acquired spectra are accurately interpreted in terms of energy and specific activity. It is achieved by performing three key tasks; peak width calibration, energy calibration, and efficiency calibration, using high quality standard spectra of appropriate geometry and source matrix (Gilmore & Hemingway, 1995). In this particular study, IAEA standard reference materials; RG-U, RG-K, RG-Th and Soil-375 were used.

The results obtained from the samples and those from certified reference materials were substituted in the comparison method formula (Equation 3.1) to get activity of the

radionuclides of interest in the sample using the Oxford PCA3 v.1 software. The software performs simultaneous fitting and identification to all the significant photo-peaks in the spectra, and displays menu driven reports that includes centroid channel energy, full width half maxima (FWHM) of identified peak, net peak area, background counts, intensity and percentage margin of uncertainty.

$$\frac{AsMs}{Is} = \frac{ArMr}{Ir} \quad \text{.....Equation 3.1 (Mohanty } et\ al.\text{, 2004)}$$

Where; M_s is the mass of the sample,

M_r is the mass of the reference material,

I_s is the intensity of the sample,

I_r is the intensity of the reference,

A_s is the activity of the sample

A_r is the activity of the reference material.

By analyzing the energy of the centroid channel and the height of a particular pulse (intensity in counts per second), the identity and activity of the nuclei that emitted the radiation are determined. Table 3.1 gives the centroid channel energies used to identify and quantify the radionuclides of interest in the samples.

Table 3.1: Recommended energy lines for gamma-ray analysis of environmental samples (IAEA, 2003)

Radionuclide	Isotope(s)	Spectral line (KeV)
K- 40	^{40}K	1460.8
Th- 232	^{212}Pb ^{228}Ac	238.6 911.2
U-238 (^{226}Ra)	^{210}Pb ^{214}Bi	351.9 609.3 1764.7
	^{210}Pb	46.5
	^{131}I	364.5

In determining the detection limits (DL) for the radionuclides, Equation 3.2 adopted from (Mohanty et al., 2004) was used, whereby the gamma-ray spectral data of the IAEA calibration standards RG-U, RG-Th and RG-K were applied.

$$\boldsymbol{DL = \frac{3C\sqrt{Bg}}{PA}} \quad \text{……...…} \quad \text{Equation 3.2 (Mohanty } \textit{et al.}\text{, 2004).}$$

Where; Bg is the background counts obtained from a gamma peak

PA is the net area under respective gamma photo peaks

C is the activity of the specific radionuclide of interest (Bq Kg^{-1})

3.4.2 EDXRF Analysis

Total elemental content in soil samples was determined using EDXRF spectrometer (Shimanzu EDX-800 HS), available at the material testing and research division of the ministry of transport and infrastructure development. The instrument had an X-ray generator consisting of an X-ray tube with Rh target that is operated at between 1 – 1000 µA and 5 – 50 kV, and a nitrogen cooled SiLi detector mounted at a 45° angle relative to the sample.

In principle, the X-ray beam generated from the X-ray tube interacts with the atoms in the sample leading to ejection of an electron (photoelectron) from the inner electron shell, leaving the atom it an excited state. A transition of an electron from the outer shell to the created vacancy occurs, with emission of an X-ray photon whose energy is equal to the energy difference between the initial and final state and characteristic of a particular element (Beckhoff et al., 2006). On the other hand, X-ray detection is performed by measuring current pulse that corresponds to an incident X-ray photon. The instantaneous current value of a single pulse is proportional to the incident X-ray energy, and thus the X-ray energy can be found by measuring the pulse height of the current pulse (Sitko and Zawisza, 2012).

The prepared soil pellets were irradiated for 100 seconds to give a spectrum. Analyses of the spectra was carried out using qualitative X-ray analyses system (QXAS) program from IAEA. Two steps were involved; spectra deconvolution and quantitative analyses of the spectra. Spectra deconvolution was done using the Analysis of X-ray spectra by Iterative Least-squares fitting (AXIL), a modular program of the IAEA‘s QXAS program. AXIL is based on the non-linear fitting of a mathematical function (describing the photopeaks and the spectral background) to experimental data (Vekemans et al., 1994). For quantitative analyses, emission-transmission method was used since the samples were of intermediate thickness (Van Grieken and Markowicz, 2001). A calibration curve was first created using samples of known element concentration, and a relationship between the element’s peak area/ intensity and the respective concentration determined. From this relationship, element concentration of an unknown sample can be determined from their peak intensities. Descriptive statistics such as mean, standard deviations, minimum and maximum of the data were then computed.

Accuracy of EDXRF analysis is dependent on identifying the peaks at their correct energy positions. This was ascertained by performing energy calibration using an internal standard A750, at least twice a week. Here, Cu-Kα position should be in the range of 8.00- 8.08 keV, where Sn-kα, Sn-Lα, Al-Kα and Ni-Kα peaks are present.

To verify the accuracy of the analytical procedure, certified reference materials (CRM) were used, and detection limits determined. For this particular study, river clay CRM from IAEA was prepared and analyzed in a similar way as the other samples. The obtained values were compared to the reported values. The lower detection limits (LDL) of various elements were also determined using Equation 3.3

$$\boldsymbol{LDL = \frac{3 * C\sqrt{Nb}}{Np}} \quad \text{..... Equation 3.3}$$

Where; *C*- Concentration of the element (mg kg^{-1}).

Np- Net peak area for the element

Nb- Net background area under the element peak.

3.5 Data Analyses

3.5.1 Potential Radiological Hazards Assessment

In this study, activity of the radionuclides and potential radiological hazards were determined. The activity of the radionuclides in the samples were determined from their respective gamma ray lines or those emitted from their decay products (Table 3.1). The gamma line of 1460.8 keV was used directly to determine ^{40}K, the weighted mean activity concentrations from gamma lines of 911.2 keV (^{228}Ac) and 583.1 keV (^{212}Pb) were used to determine ^{232}Th, and the gamma lines of 295.2 keV (^{214}Pb), 609.3 keV (^{214}Bi), and 186.1 keV (^{226}Ra) were used to determine ^{226}Ra from their weighted mean activity. On the other hand, radiological hazards due to γ-ray radiation were assessed using radium equivalent activity (Ra_{eq}), Gamma index ($I_{\gamma r}$) and external hazard index, using Equation 3.4, Equation 3.5 and Equation 3.6 (Bashir et al., 2012) respectively.

$$\mathbf{Ra_{eq} = A_U + 1.43\ A_{Th} + 0.077\ A_K}$$ ……. Equation 3.4

$$\mathbf{I_{yr} = (1/150)\ A_U + (1/100)\ A_{Th} + (1/1500)\ A_K}$$ ……...…. Equation 3.5

$$\mathbf{H_{ex} = (A_U/\ 370) + (A_{Th}/259) + (A_K/4810)}$$ …….. Equation 3.6

Where; A_U-Specific activities of ^{238}U in Bq kg^{-1}

A_{Th}- Specific activities of, ^{232}Th in Bq kg^{-1}

A_K- Specific activities of ^{40}K in Bq kg^{-1}

3.5.2 Absorbed dose rate and annual effective dose determination

The absorbed dose rate in air (D), at 1 m from terrestrial sources of gamma radiation in the soil samples were estimated from the results of the activity of the radionuclides; ^{40}K, ^{232}Th and ^{238}U, using Equation 3.7, which was adopted from UNSCEAR (1993).

$$\mathbf{D = 0.427\ A_U + 0.662\ A_{Th} + 0.043\ A_k}$$ …… Equation 3.7

The annual effective dose (E) due to the natural radionuclides in the soil samples was estimated using Equation 3.8 (UNSCEAR, 1993). A dose conversion coefficient (Q) of 0.7 Sv Gy^{-1} to convert the absorbed dose rate in air to the effective dose, and the outdoor occupancy factor (f) of 0.2, proposed by UNSCEAR, (2000) were used.

$$\mathbf{E = T*f*Q*D}$$ …… Equation 3.8

Where; T = total seconds per year ≈ 8760.

Chapter Four

Results And Discusion

4.0 Introduction

In this chapter, the results of the study are presented and discussed. This includes quality assurance results, elemental content and radioactivity levels.

4.1 Precision and Accuracy of the Results

For the purpose of this study, two analytical methods were used i.e. gamma spectroscopy and energy dispersive x-ray fluorescence (EDXRF) spectroscopy. Certified reference materials were used to assess the accuracy and reliability of these analytical methods.

4.1.1 Accuracy of EDXRF Spectroscopy Method

To assess the accuracy of EDXRF analytical method, PTXRF-IAEA09 river clay certified reference material was used. The results obtained were compared with the certified values provided in the certificate (Table 4.1). The measured values of most of the elements of interest were found to be within the certified range, apart from Cu, where slightly higher values were recorded, and Ni, with slightly lower values being recorded. However, using two tailed student t-test, the difference between the measured mean from the certified mean was found to be insignificant at 95% confidence limit. This was a good indication of the accuracy and reliability of the method used.

From the results of certified reference material, detection limits were also determined using Equation 3.3, as presented in Table 4.2. In general, the detection limit improved with increasing atomic number.

Table 4.1: Results of the analyses of PTXRF-IAEA09 river clay

Element	**Experimental values** **mg kg^{-1}**	**Certified Range** **(90% C.I.)**
Ti	4737 ± 214	4100 - 4500
Mn	1055 ± 60	940 - 1060
Fe	30750 ± 1550	28700 - 30700
Ni	31 ± 5	35 - 40
Cu	28 ± 4	18 - 22
Zn	86 ± 12	88 - 103
Sr	94 ± 7	97 - 114
Zr	297 ± 14	281 - 322

Table 4.2: Detection limits of various elements using EDXRF spectroscopy

Element	Detection Limit (mg kg^{-1})
Ti	500
Mn	120
Fe	70
Zn	20
Sr	15
Zr	12
Nb	10
Pb	5

4.1.2: Accuracy of Gamma Spectroscopy

To determine the activity of radionuclides, three IAEA standard reference materials of known activity were used; RG-K, RG-Th and RG-U for ^{40}K, ^{232}Th and ^{238}U peaks, respectively. The results obtained from these standards (Table 4.3) were substituted in the comparison method formula (Equation 3.1), to get activity of the radionuclides of interest.

To assess the accuracy of gamma spectroscopy for the analyses, IAEA-375 certified reference material was used. The obtained results were found to fall within the certified range (Table 4.4).

Table 4.3: Results of analyses of RG-K, RG-Th and RG-U standard reference material

Standard	Nuclide	Energy (keV)	Activity (mg kg^{-1})
RG-K	^{40}K	1461	14000
RG-TH	^{232}Th	238	3250
		912	3250
RG-U	^{238}U	351	4940
		609	4940

Table 4.4: Results of analyses of IAEA-375 certified reference material

IAEA-375	Average Activity ($Bq\ kg^{-1}$)	Certified Activity Range (90% CI)
^{232}Th	18 ± 2	19 - 22
^{238}U	17 ± 3	19 - 29
^{40}k	445 ± 12	417 - 432

4.2 Elemental content

Elemental analyses of the collected soil samples were done using EDXRF. Concentration levels of heavy metals (Fe, Ti, Mn, Zn, Sr and Pb), rare earth elements (Nb, Y and Ce), and radionuclides (Th and U), were determined.

4.2.1 Heavy Metals

The mean concentration levels of various heavy metals in soil samples are presented in Table 4.5. The highest concentration levels were recorded for Fe, Mn and Ti. Zn, Pb and Sr were also recorded above detection limits.

Iron

High concentration levels of Fe were recorded in all the soil samples, within a range of 14 to 47%, and an overall mean of 29%. These values are higher than those recorded by Patel and Mangala (1994), where a concentration range of 5% to 30%, with a mean of 21% was recorded. The increment could be attributed to enhanced prospective and small scale mining activities. These activities are through open cast mining that could lead to elements in the lower soil profile finding their way to the topsoil. In a study by Maina (2008), in a neighboring titanium mining site, iron was determining at a range of 0.09% to 3.1%, while levels as high as 58% were recorded by Achola et al. (2012).

For Fe to be commercially viable for exploration, the Fe content must be high, with low impurity content. Three classifications are generally used for iron ore, based on the percentage Fe content i.e. High grade ore (above 65%), Medium grade ore (62 – 64%),

and Low grade ores at below 58% (Muwaguzi et al., 2012). Although the Fe content in the analyzed samples falls in the last category, it's worth noting that the samples were representative of the topsoil.

Titanium

Ti was found to be a major constituent in all the soil samples collected for this study. A concentration range of between 1.1 to 8.3%, and a mean of 3.5% were recorded. Almost a similar range was observed by Patel and Mangala (1994), where a concentration range of 1% to 9%, and a mean concentration of 4.9% was recorded, while lower concentration values between 0.1% to 2.8% and a mean range 1.2 ± 0.2%, were recorded by Maina (2008).

Manganese

Mn was found to be the second most abundant element after iron in most of the soil samples, with an overall mean of 7.4%. The highest concentration levels was determined at 18% while the minimum at 0.5%. In a previous study by Patel and Mangala (1994), manganese was determined at 0.4% to 17%, with a mean of 6.3%, therefore no significant change between the two studies. However, unlike the present study where fine topsoil were used, Patel and Mangala (1994) mainly used rock samples, thus the high concentration levels recorded could be as a result of rock weathering.

Zinc

The mean concentration of Zn in soil samples ranged from 94 - 2549 mg kg^{-1}, with a mean of 1587 mg kg^{-1}. These levels are above worldwide range in contaminated soil (150- 300 mg kg^{-1}), as well as regulatory limits at 500 mg kg^{-1} (Yadav, 2010). Lower concentration levels have been recorded in a study by Achola et al. (2012) in a high radiation background area, southwestern Kenya, where Zn levels varied between 166 - 1850 mg kg^{-1}.

Lead

Pb has no known physiological role in human health. Therefore, even at low concentration levels, Pb is usually considered a potential health hazard. In this study, concentration levels varied from 205 – 2661 mg kg^{-1}, and an overall mean of 1023 mg kg^{-1}. These levels are very high compared worldwide average for surface soils of 32 mg kg^{-1} (Wuana & Okieimen, 2011). Concentration range between 56 – 1560 mg kg^{-1} was reported by Achola et al. (2012).

Zirconium and Strontium

Zr and Sr were determined at levels above detection limits as shown in Table 4.5. For Sr, a concentration range of between 551 – 6606 mg kg^{-1} was recorded, with an overall mean of 3399 mg kg^{-1}. These levels are much higher than the estimated global abundance in soils at 200 – 300 mg kg^{-1} (ATSDR, 2004). Due to its chemical similarities with calcium, Sr is easily absorbed in human body. At such high levels, Sr can pose a significant health risk, particularly to the infants and young children. Some of the health effects associated with Sr includes bone toxicity and cancer (WHO, 2010). On the other hand, high Zr levels in the soil samples were recorded, ranging from 142 - 872 mg kg^{-1}. These levels are comparable to those reported by Patel and Mangala (1994), as well as within the natural concentration range in soil of 32 – 850 mg kg^{-1} (Fodor et al., 2005; Kabata-Pendias, 2001).

Table 4.5: Heavy metal content in soil samples

	Ti (W %)	Mn (W %)	Fe (W %)	Zn (mg kg^{-1})	Sr (mg kg^{-1})	Zr (mg kg^{-1})	Pb (mg kg^{-1})
S1	3.5 ± 0.2	4.9 ± 0.2	23±1.1	1052 ± 58	2046 ± 60	594 ± 18	492 ± 30
S2	2.5 ± 0.1	1.2 ± 0.1	16±0.8	667 ± 44	1922 ± 52	516 ± 15	270 ± 19
S3	5.5 ± 0.3	10 ± 0.4	39±1.6	1813 ± 84	3580 ± 102	645 ± 20	979 ± 53
S4	4.8 ± 0.3	4.9 ± 0.2	37±1.5	2006 ± 114	6192 ± 161	524 ± 19	482 ± 35
S5	5.8 ± 0.3	12 ± 0.5	47±2.0	2191 ± 106	6606 ± 199	377 ± 20	594 ± 41
S6	5.6 ± 0.3	5.3 ± 0.2	38±1.7	2000 ± 104	4496 ± 131	590 ± 21	535 ± 34
S7	4.6 ± 0.2	5.9 ± 0.2	35±1.6	1706 ± 86	3518 ± 105	872 ± 27	599 ± 36
S8	5.9 ± 0.3	3.8 ± 0.1	35±1.4	1195 ± 61	3967 ± 103	683 ± 22	532 ± 36
S9	5.7 ± 0.3	3.7 ± 0.1	32 ±1.3	1619 ± 81	4022 ± 103	683 ± 20	530 ± 38
S12	5.8 ± 0.3	7.6 ± 0.3	43±2.0	2007 ± 113	4024 ± 131	647 ± 23	681 ± 48
S13	4.9 ± 0.3	8.0±0.4	44±2.1	1792 ± 96	3350 ± 112	559 ± 20	560 ± 39
S14	3.4 ± 0.1	7.1 ± 0.2	45 ±1.4	2269 ± 92	2784 ± 66	524 ± 16	457 ± 32
S15	4.3 ± 0.2	6.4 ± 0.1	37±0.6	1970 ± 58	5086 ± 82	467 ± 19	713 ± 43
S16	4.6 ± 0.3	6.4 ± 0.3	31 ±1.4	1483 ± 89	4327 ± 137	460 ± 19	857 ± 50
S17	2.5 ± 0.3	9.3 ± 0.3	27 ±0.9	1550 ± 71	3113 ± 76	279 ± 16	973 ± 52
S18	3.5 ± 0.3	12 ± 0.4	31 ±1.2	2036 ± 112	2625 ± 92	408 ± 20	751 ± 48
S19	2.3 ± 0.3	13 ± 0.4	33±1.0	1783 ± 75	2376 ± 61	381 ± 14	1321 ± 63
S20	1.3 ± 0.1	0.5 ± 0.1	16 ±2.0	577 ± 81	6069 ± 674	338 ± 40	2661 ± 344
S21	4.9 ± 0.34	7.8 ± 0.3	34 ±1.6	1564 ± 87	3537 ± 113	635 ± 22	942 ± 55
S22	1.4 ± 0.2	5.0 ± 0.1	22±0.3	1135 ± 47	2473 ± 44	302 ± 12	1848 ± 66

Table 4.5: Heavy metal content in soil samples (Cont'd)

	Ti (W %)	Mn (W %)	Fe (W %)	Zn (mg kg^{-1})	Sr (mg kg^{-1})	Zr (mg kg^{-1})	Pb (mg kg^{-1})
S23	2.4 ± 0.7	14 ± 0.5	32 ± 1.2	1906 ± 96	2694 ± 76	366 ± 15	1276 ± 67
S24	1.5 ± 0.5	7.1 ± 0.3	26 ± 1.1	1398 ± 80	2484 ± 79	224 ± 13	1619 ± 93
S25	3.7 ± 0.4	9.0 ± 0.3	36 ± 1.1	2327 ± 98	4149 ± 105	333 ± 17	1008 ± 53
S26	2.3 ± 0.3	11 ± 0.3	29 ± 0.9	2170 ± 106	3177 ± 90	319 ± 15	1246 ± 62
S27	2.4 ± 0.3	1.3 ± 0.2	31 ± 1.5	1524 ± 91	2256 ± 81	326 ± 17	1478 ± 87
S28	1.7 ± 0.2	6.0 ± 0.3	19 ± 1.1	930 ± 60	2591 ± 89	310 ± 16	1094 ± 67
S29	1.0 ± 0.3	5.5 ± 0.1	22 ± 0.3	1111 ± 44	2680 ± 45	228 ± 12	1484 ± 58
S30	1.4 ± 0.4	5.3 ± 0.1	22 ± 0.3	1543 ± 53	4290 ± 68	142 ± 13	2222 ± 86
S31	2.6 ± 0.4	7.8 ± 0.1	31 ± 0.4	1045 ± 50	4412 ± 72	194 ± 15	1202 ± 58
S32	2.0 ± 0.4	7.2 ± 0.1	24 ± 0.5	1379 ± 54	2862 ± 58	305 ± 13	1859 ± 69
S33	1.1 ± 0.2	5.7 ± 0.5	14 ± 1.3	1227 ± 113	2501 ± 155	198 ± 15	2007 ± 135
S34	3.1 ± 0.3	10 ± 0.4	30 ± 1.4	2549 ± 134	2607 ± 90	472 ± 19	985 ± 59
S35	1.6 ± 0.3	12 ± 0.3	23 ± 0.5	1759 ± 62	2745 ± 59	240 ± 15	923 ± 49
S36	1.5 ± 0.3	18 ± 0.2	27 ± 0.4	1708 ± 57	2310 ± 41	228 ± 11	975 ± 52
S37	1.4 ± 0.3	10 ± 0.2	25 ± 0.3	1736 ± 62	2044 ± 37	195 ± 11	1392 ± 53
S38	2.4 ± 0.1	6.3 ± 0.2	21 ± 0.9	1189 ± 62	3217 ± 90	321 ± 12	661 ± 37
S39	3.8 ± 0.2	2.1 ± 0.1	25 ± 1.1	622 ± 76	3687 ± 89	577 ± 17	298 ± 22
S40	5.5 ± 0.3	7.8 ± 0.2	34 ± 1.1	2291 ± 104	3441 ± 87	542 ± 19	1038 ± 54

Niobium

Naturally, Nb occurs in soil at smaller quantities in comparison to other heavy metals such as Ti, Fe and Mn, at a global average of 10 – 20 mg kg^{-1} (Dill, 2010; Kabata-Pendias, 2001). However, considering that the sampling area for this particular study was in a Nb mining site, high levels of Nb were anticipated. This proved to be the case, with levels of up to 7511 mg kg^{-1} being recorded. In a previous study by Patel and Mangala (1994), a mean of 4062 mg kg^{-1} was reported.

4.2.2 Rare Earth Elements

Y, Ce and Zr were identified above detection limits in all the soil samples (Table 4.6). Cerium was found to be the most abundant of the three at a range of 0.7% - 7.9%, and a mean of 3.8%. This is way above the average soil content at 70 mg kg^{-1}. The mean concentration of Y was 813 mg kg^{-1}, whilst Zr was determined at 429 mg kg^{-1}. The levels recorded for the three rare earths are high as compared to the normal range in soils. This observation can be associated with the huge deposits of these elements in the region.

4.2.3 Radionuclides

While Th was detected in all soil samples, U was recorded below detection limits in some sites. Th concentration ranged from 28 – 879 mg kg^{-1}, which is comparable to values reported by Achola et al. (2012), at a range of 25 - 1346 mg kg^{-1} in a high radiation background region. On the other hand, U ranged from BDL (<10) to 86 mg kg^{-1}.

Table 4.6: Concentration levels of Y, Nb, Ce, Th and U

Site	Y (mg kg^{-1})	Nb (mg kg^{-1})	Th (mg kg^{-1})	U (mg kg^{-1})
S1	407 ± 13	1464 ± 37	258 ± 17	< 10
S2	454 ± 15	1266 ± 31	202 ± 12	< 10
S3	622 ± 19	2570 ± 62	462 ± 26	25 ± 7
S4	1184 ± 31	3017 ± 67	334 ± 20	86 ± 11
S5	1915 ± 55	3836 ± 96	424 ± 30	84 ± 10
S6	1160 ± 33	3661 ± 88	380 ± 23	44 ± 8
S7	842 ± 26	3639 ± 91	346 ± 23	26 ± 7
S8	799 ± 22	3523 ± 77	274 ± 18	29 ± 7
S9	695 ± 19	3093 ± 67	289 ± 19	39 ± 9
S11	100 ± 5	237 ± 8	50 ± 6	41 ± 6
S12	999 ± 32	4241 ± 115	425 ± 28	39 ± 7
S13	832 ± 30	3752 ± 103	328 ± 24	37 ± 8
S14	1130 ± 28	4534 ± 91	259 ± 20	33 ± 7
S15	1145 ± 22	4266 ± 66	388 ± 22	50 ± 9
S16	925 ± 31	2256 ± 61	454 ± 25	51 ± 7
S17	434 ± 14	1850 ± 41	350 ± 20	18 ± 7
S18	519 ± 18	1824 ± 46	343 ± 22	32 ± 9
S19	464 ± 15	1675 ± 38	704 ± 39	19 ± 6
S20	2976 ± 322	3276 ± 335	691 ± 87	83 ± 14
S21	497 ± 18	2679 ± 71	437 ± 27	38 ± 8
S22	815 ± 19	2467 ± 40	879 ± 36	<10
S25	701 ± 20	2998 ± 66	479 ± 28	35 ± 7
S26	704 ± 22	2726 ± 66	433 ± 23	<10
S27	428 ± 18	1853 ± 59	415 ± 26	<10
S28	330 ± 13	1806 ± 55	426 ± 31	19 ± 6
S29	939 ± 22	2283 ± 38	754 ± 37	<10
S30	1005 ± 22	2632 ± 44	771 ± 36	<10
S31	1491 ± 30	7511 ± 113	712 ± 39	39 ± 9
S32	386 ± 14	1781 ± 33	405 ± 21	19 ± 7
S33	532 ± 33	1904 ± 99	607 ± 43	<10
S34	551 ± 22	1849 ± 55	423 ± 27	28 ± 7
S35	382 ± 13	1578 ± 35	440 ± 23	<10
S36	403 ± 12	1836 ± 31	407 ± 26	<10
S37	488 ± 13	1694 ± 31	592 ± 28	<10
S38	438 ± 14	1839 ± 44	289 ± 16	<10
S39	865 ± 22	1359 ± 49	230 ± 15	44 ± 7
S40	448 ± 16	1665 ±40	338 ± 19	<10

4.3 Activity

Table 4.6 gives the activity of radionuclide ^{232}Th, ^{238}U and ^{40}K in soil samples from Mrima Hill. The highest activity was reported for ^{232}Th, followed by ^{40}K and ^{238}U (Figure 4.1). The activity ranged from; 124 – 4246 Bq kg^{-1} with a mean of 1400 ± 795Bq kg^{-1} for ^{232}Th; 42 – 469 Bq kg^{-1}, with a mean of 143 ± 11 Bq kg^{-1} for ^{238}U; and 42 – 482 Bq kg^{-1} with a mean of 200 ± 92 Bq kg^{-1} for ^{40}K. Relative to other sites, exceptionally high value for ^{232}Th was recorded in site S10. In addition, high ^{40}K activity concentrations were also recorded from this site. This could be attributed to the nature of the sample, whereby, unlike the others, sample S10 was a rock sample.

The activity values recorded in this study are higher than the global mean of ^{238}U and ^{232}Th at 35 Bq kg^{-1} and 30 Bq kg^{-1} respectively (UNSCEAR 2000). However, these values are comparable to those obtained in other high radiation background areas in Kenya. Achola et al. (2012), obtained a mean activity of 178 Bq kg^{-1} and 1396 Bq kg^{-1} for ^{238}U and ^{232}Th respectively, while Otwoma et al. (2013), reported a range of 17 - 1447 Bq kg^{-1} and 23 - 1369 Bq kg^{-1} for ^{238}U and ^{232}Th respectively.

Values below the worldwide average of 400 Bq kg^{-1} (UNSCEAR, 2000), were recorded for ^{40}K. Additionally, these values are lower than those reported in previous studies (Achola et al., 2012; Otwoma et al., 2013). Contrary to the trends observed in the present study, the two studies found ^{40}K to be the major contributor to exposure levels, whereby, activity concentration of ^{40}K was found to be much higher than ^{232}Th and ^{238}U. This observation could be attributed to low natural potassium concentrations in soil around Mrima Hill, where a mean of 3290 µg g^{-1} was recorded, with a number of sites reporting values below detection limit.

Table 4.7: Activity of ^{232}Th, ^{238}U and ^{40}K in Bq kg^{-1}

Sample Code	^{232}Th	^{238}U	^{40}K
S1	402 ± 6	52 ± 3	482 ± 21
S2	676 ± 7	125 ± 4	398 ± 19
S3	1376 ± 10	105 ± 9	189 ± 18
S4	1184 ± 8	399 ± 5	216 ± 16
S5	1293 ± 9	344 ± 3	148 ± 5
S6	1200 ± 9	226 ± 5	170 ± 16
S7	1227 ± 5	193 ± 6	161 ± 8
S8	983 ± 8	170 ± 4	149 ± 14
S9	1058 ± 6	161± 4	152 ± 11
S10	4246 ± 12	157 ± 6	427 ± 20
S11	124 ± 2	76 ± 7	42 ± 5
S12	1405 ± 8	195 ± 9	181 ± 13
S13	1003 ± 13	215 ± 7	127 ± 23
S14	732 ± 30	311 ± 6	129 ± 9
S15	1036 ± 10	271 ± 5	110 ± 18
S16	1523 ± 12	140 ± 5	208 ± 20
S17	1324 ± 69	110 ± 3	194 ± 11
S18	1151 ± 53	76 ± 6	183 ± 10
S19	2147 ± 18	68 ± 8	223 ± 14
S20	2197 ± 10	469 ± 5	257 ± 18
S21	1361 ± 63	108 ± 9	175 ± 10
S22	2424 ± 85	84 ± 3	261 ± 13

Table 4.7: Activity of ^{232}Th, $^{238}U$and ^{40}K in Bq kg^{-1} (Cont'd)

Sample Code	^{232}Th	^{238}U	^{40}K
S23	1667 ± 12	87 ± 55	193 ± 20
S24	1755 ± 75	42.2 ± 32	228 ± 12
S25	1254 ± 84	103 ± 4	168 ± 14
S26	1093 ± 6	58 ± 7	171 ± 10
S27	1356 ± 76	93 ± 4	158 ±14
S28	1509 ± 74	98 ± 4	202 ± 12
S29	2184 ± 62	68 ± 7	247 ± 10
S30	1610 ± 68	89 ± 4	208 ± 12
S31	1525 ± 11	56 ± 5	199 ± 19
S32	1111 ± 6	63 ± 7	149 ± 10
S33	1557 ± 10	50 ± 4	201 ± 17
S34	1190 ± 11	84 ± 5	158 ± 19
S35	1537 ± 78	106 ± 4	189 ± 14
S36	1316 ± 87	103 ± 4	237 ± 15
S37	2172 ± 11	94 ± 5	253 ± 19
S38	1048 ± 7	93 ± 3	147 ± 11
S39	1020 ± 51	300 ± 3	158 ± 9
S40	1021 ± 71	90 ± 3	140 ± 12
Average	**1400 ± 795**	**143 ± 111**	**200 ± 92**
Maximum	**4246 ± 12**	**469 ± 5**	**482 ± 21**
Minimum	**124 ± 2**	**42 ± 3**	**42 ± 5**

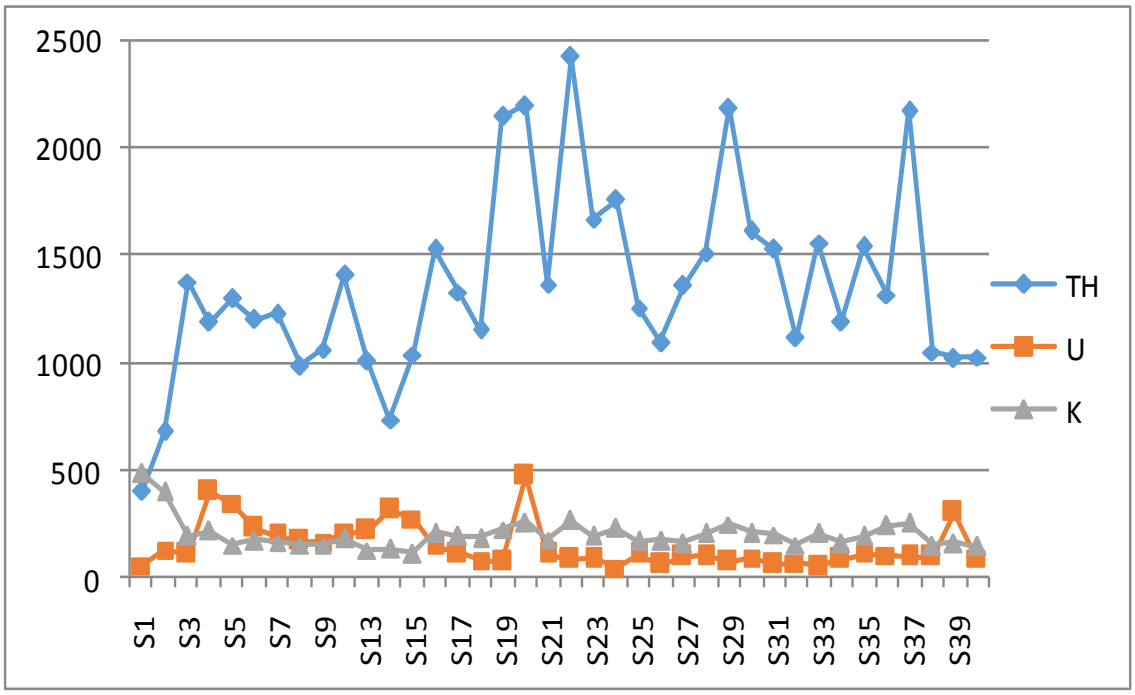

Figure 4.1: Trends and distribution patterns of ^{232}Th, ^{238}U and ^{40}K in soils around Nb mining site in Kwale County.

A good positive correlation was observed between the elemental concentrations and activity of ^{40}K, ^{232}Th and ^{238}U as shown in Figure 4.2, 4.3 and 4.4, respectively. The obtained correlation coefficient is 0.78 for ^{232}Th, 0.39 for ^{40}K and 0.71 for ^{238}U. Therefore, elemental concentration levels especially for thorium and uranium can be used as an indicator for activity levels and vice versa. IAEA (1989) proposed the following conversion factors;

1% K = 313 Bq kg^{-1} of ^{40}K

1 ppm U = 12.35 Bq kg^{-1} of ^{238}U

1 ppm Th = 4.06 Bq kg^{-1} of ^{232}Th

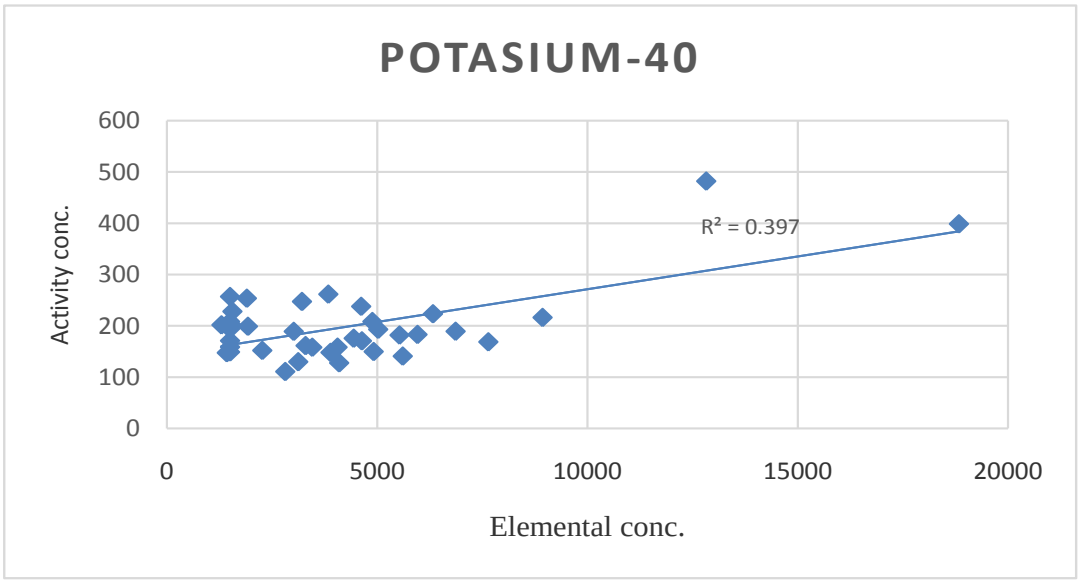

Figure 4.2 Correlation analyses between elemental concentration and activity levels for ^{40}K (Table 4.6 and 4.7).

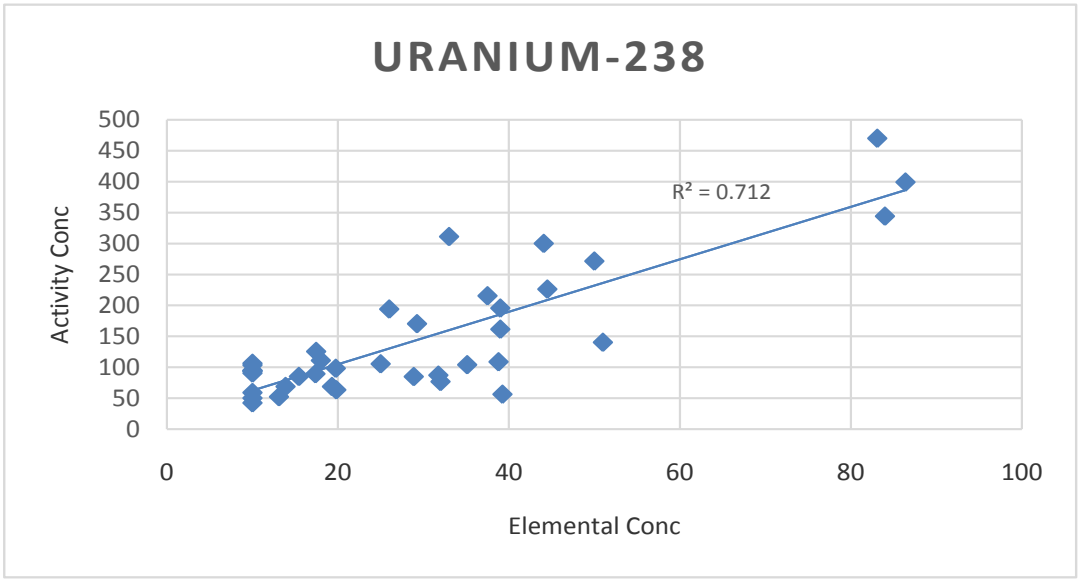

Figure 4.3: Correlation analyses between elemental concentration and activity levels for ^{238}U (Table 4.6 and 4.7).

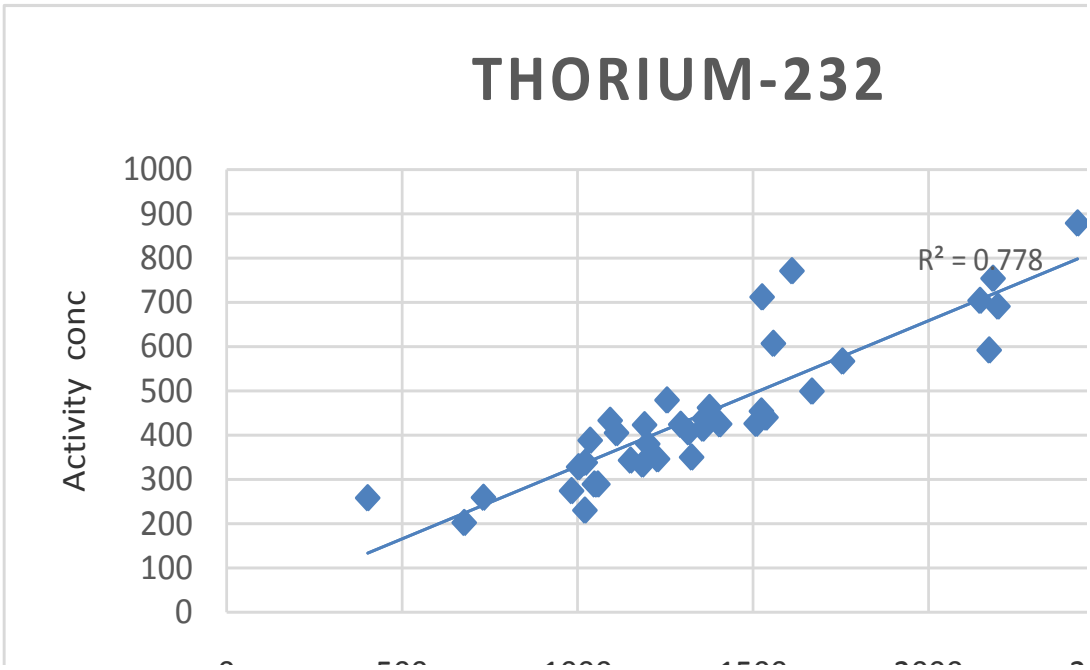

Figure 4.4: Correlation analyses between elemental concentration and activity levels for ^{232}Th (Table 4.6 and Table 4.7).

Figure 4.5, 4.6 and 4.7 shows the correlation between activity concentrations of (i) ^{238}U and ^{40}K; (ii) ^{238}U and ^{232}Th; and (iii) ^{40}K and ^{232}Th, respectively. A negative correlation was observed between ^{40}K and ^{238}U, as well as between ^{238}U and ^{232}Th, with a correlation coefficient of -0.40 and -0.51 respectively. On the other hand, a strong positive correlation between ^{232}Th and ^{40}K was recorded with a correlation coefficient of 0.72.

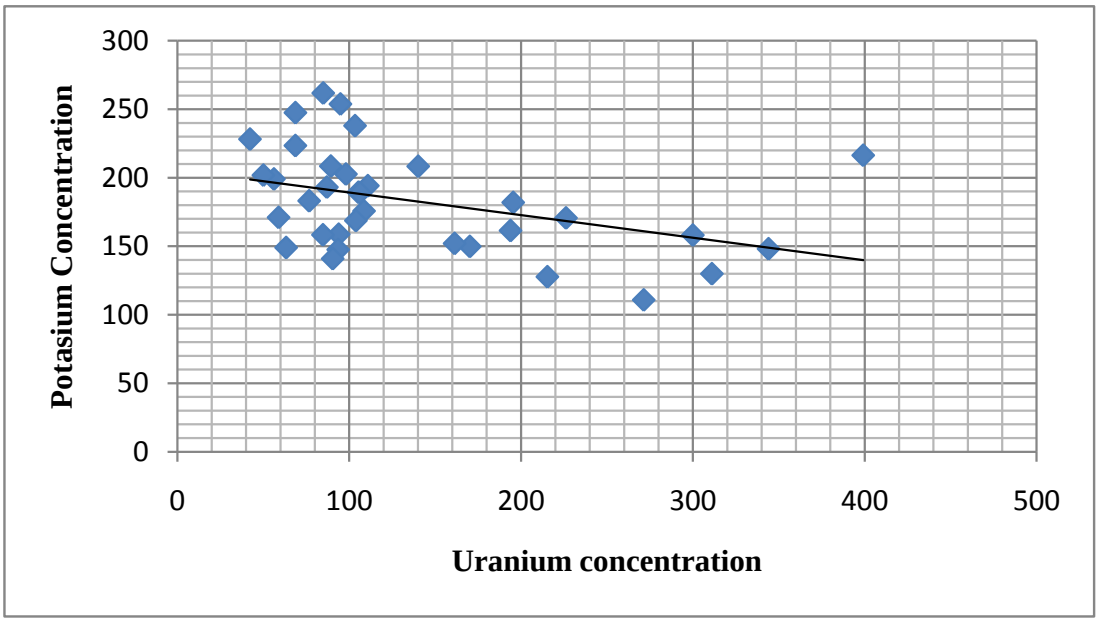

Figure 4.5: A graph showing how activity of ^{238}U correlates to that of ^{40}K in the study area (Table 4.7).

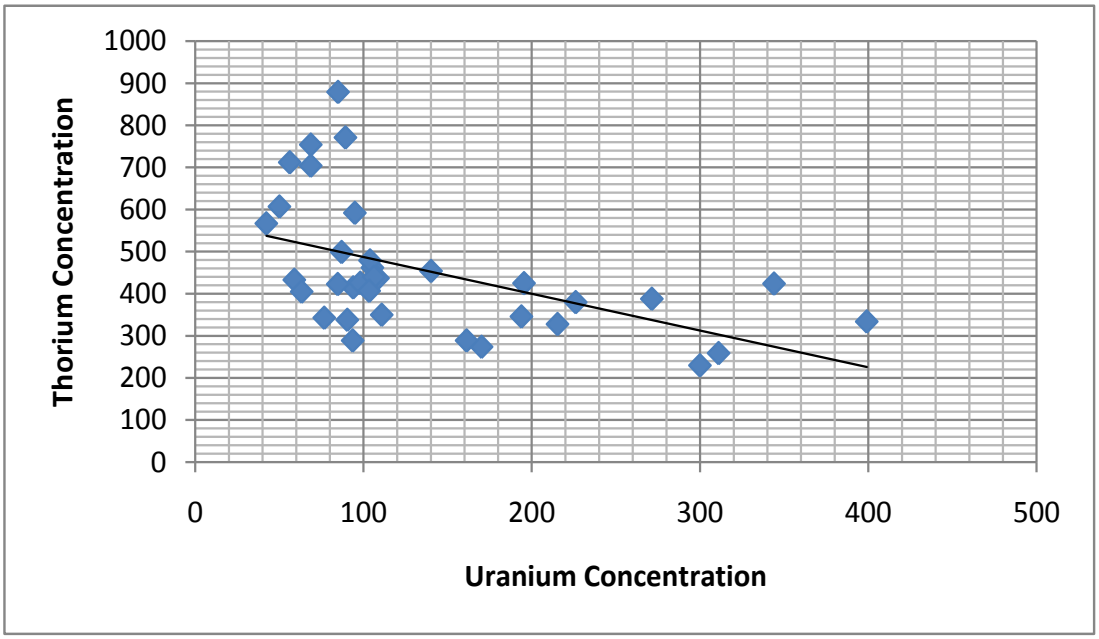

Figure 4.6: A graph showing how activity of ^{238}U correlates to that of ^{232}Th in the study area (Table 4.7).

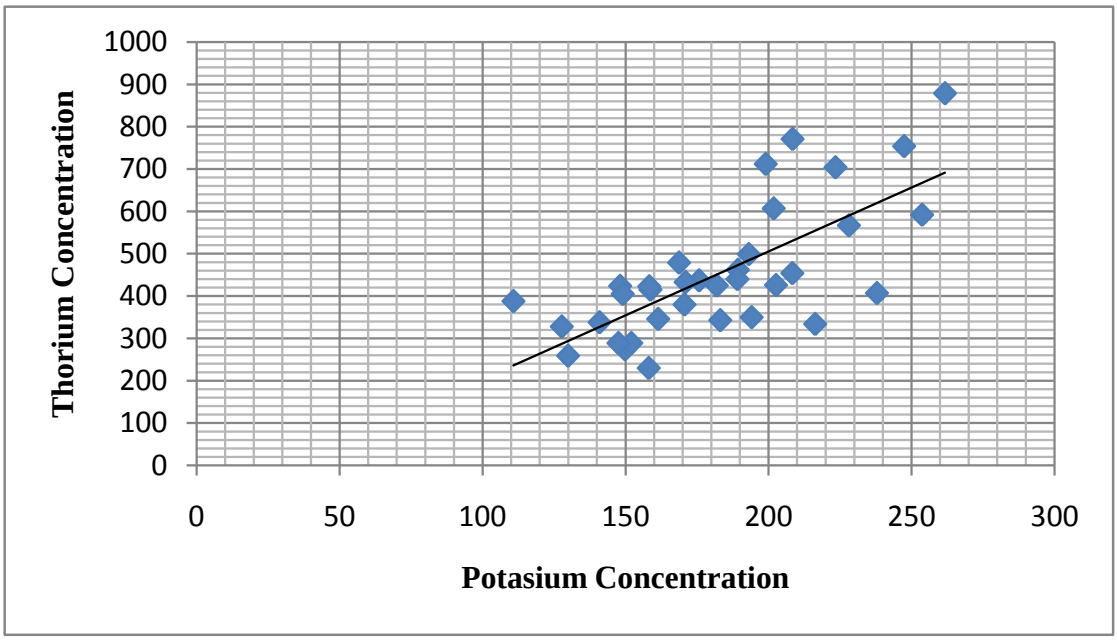

Figure 4.7: A graph showing how activity of ^{40}K correlates with those of ^{232}Th in the study area (Table 4.7).

4.4 Evaluation of Radiological Hazards

To understand the radiological hazards posed to residents and workers around Mrima Hill, radium equivalent (Ra_{eq}), external hazard index (H_{ex}), Representative gamma index (I_{yr}), Absorbed dose rate (D) and annual effective dose (E) were calculated using activity concentration of ^{238}U, ^{232}Th and ^{40}K (Table 4.7).

Absorbed Dose Rate

The absorbed dose rate in air, 1m from the ground surface were estimated from the results of the activity concentration of the radionuclides using Equation 3.7. The absorbed dose rate estimates are presented in column V of Table 4.7. An estimated dose rate of between 309 - 2896 nGy h^{-1} was obtained, with a mean of 997 ± 524 nGy h^{-1}. Therefore, all the sampled areas recorded dose values at least five times higher than the global average of 60 nGy h^{-1} (UNSCEAR, 2000). In similar studies, Achola et al. (2012) obtained an average absorbed dose value of 2300 nGy h^{-1} in a high background area in Southwestern Kenya,

while Mohanty et al. (2004), reported to range between 650 to 3150 nGy h^{-1} in India. Odumo et al. (2011) obtained a lower mean dose value of 142 nGy h^{-1}. However, the calculated values do not take into account the contribution from cosmic rays.

Annual Effective Dose

The calculated annual effective dose in Mrima Hill are presented in column VI in Table 4.7. The obtained values ranged from 379 µSv y^{-1} to 3552 µSv y^{-1}, with a mean value of 1222 ± 643 µSv y^{-1}. The obtained values are higher than the mean annual effective dose from natural radionuclides at 460 µSv y^{-1} as per UNSCEAR (1993), an indicator that Mrima Hill is a high background radiation area. These estimated values are lower than the range obtained by Achola et al. (2012), between 1716 to 14716 µSv y^{-1} with a mean value of 5704 ± 3442 µSv y^{-1}, but higher than annual effective dose rate obtained in a nearby titanium mines at a range of 24 - 84 µSv y^{-1} by Maina (2008).

Radium Equivalent

To determine the gamma radiation hazards associated with the use of the soil from the mining sites in construction, radium equivalent activity (Ra_{eq}) was calculated using the obtained activity. The Ra_{eq} is related to the external dose and internal dose due to radon and its daughters. In this study, the estimated radium equivalent activity ranged from 664 to 6262 Bq kg^{-1}, with an overall mean of 2161±1133 Bq kg^{-1}. These calculated values are much higher than maximum permissible limits at 370 Bq kg^{-1}, as per IAEA recommendation. In comparison to other related studies, a lower mean value of 132 Bq $kg^{-1}$was recorded by Ademola et al. (2014).

Table 4.8 Estimated values for radium equivalent dose, external hazard index, absorbed dose rate and annual effective dose

	Ra_{eq} (Bq kg^{-1})	**I_{yr}**	**D** (nGy h^{-1})	**E** (µSv y^{-1})
S1	664	4.6	309	379
S2	1123	7.8	518	636
S3	2087	14	964	1182
S4	2109	14	963	1182
S5	2205	15	1009	1238
S6	1955	13	898	1101
S7	1961	13	902	1106
S8	1588	11	730	895
S9	1686	11	775	951
S10	6262	43	2896	3552
S11	258	1.7	117	143
S12	2219	15	1021	1253
S13	1659	11	761	934
S14	1368	9	623	764
S15	1761	12	806	989
S16	2335	16	1077	1321
S17	2020	14	932	1143
S18	1737	12	802	984
S19	3156	22	1460	1790
S20	3632	25	1666	2044
S21	2068	14	955	1171
S22	3572	24	1652	2026
S23	2486	17	1149	1409

Table 4.8: Estimated values for Ra equivalent dose, external hazard index, representative gamma index, absorbed dose rate and annual effective dose (Cont'd)

	Ra_{eq} (Bq kg^{-1})	**I_{yr}**	**H_{ex}**	**D** (nGy h^{-1})	**E** (µSv y^{-1})
S24	2569	17	6.9	1189	1459
S25	1911	13	5.1	882	1082
S26	1635	11	4.4	756	927
S27	2046	14	5.5	944	1158
S28	2272	15	6.1	1049	1287
S29	3211	22	8.6	1486	1822
S30	2408	16	6.5	1113	1365
S31	2253	15	6.0	1042	1278
S32	1663	11	4.4	769	943
S33	2293	16	6.1	1061	1301
S34	1799	12	4.8	831	1019
S35	2319	16	6.2	1071	1313
S36	2004	14	5.4	925	1135
S37	3221	22	8.6	1489	1827
S38	1604	11	4.3	740	908
S39	1772	12	4.7	810	994
S40	1562	10	4.2	720	884
Average	**2161 ± 1133**	**15 ± 7**	**5.8 ± 3.1**	**997 ± 524**	**1222 ± 643**
Max	**6262**	**43**	**16**	**2896**	**3552**
min	**664**	**4.69**	**1.7**	**309**	**379**

Representative Gamma Index

Representative gamma index (I_{yr}) is an estimation of the level of gamma radioactivity associated with different concentrations of specific radionuclides ^{232}Th, ^{40}K and ^{238}U, and is calculated using Equation 3.4, whereby, values of $I_{yr} \leq 1$ corresponds to an annual effective dose of less than or equal to 1 mSv.

The obtained estimate values are presented in Table 4.7. These values varied from 4 to 43, with an average of 15 ± 7. The results show that all the values are above the limit of unity, which implies that the radiation dose is above permissible limit of 1 mSv y^{-1}. Therefore, from representative gamma index as well as other calculated indices in this study, it can be concluded that there are significant radiological health risks to the people living in and around Mrima Hill.

Chapter Five

Conclusions And Recommendations

5.1 Conclusions

The elemental and activity levels in soil samples from Mrima hill were determined using EDXRF and HPGe gamma spectroscopy, respectively. From the results of certified reference materials, these two techniques proved reliable for the task.

Most elements were determined at concentration levels above the recommended limits in agricultural soils. For instance, Fe, Mn and Ti were found to be the major constituent in the soil samples with mean concentration of 29%, 7.4% and 3.4% respectively. Other soil constituents include Zn (94 - 2549 µg g^{-1}), Pb (205 – 2661 µg g^{-1}) and Sr (551 – 6606 µg g^{-1}). Nb concentrations were also found to be much higher than the normal range in soils, at a range of 151 – 7511 µg g^{-1}. Similar observations were made with respect to rare earth elements i.e. Y (100 – 2776 µg g^{-1}) and Zr (142 – 542 µg g^{-1}). These values can be associated with the huge mineral deposits, particularly niobium and rare earths, discovered in the region. These results are however comparable to a previous study conducted in the area.

The activity as a result of NORMS i.e. ^{232}Th, ^{238}U and ^{40}K, indicted that Mrima Hill is a high background radiation area. Activity above world average were reported. The mean activity was reported at 1400 ± 795 Bq kg^{-1} for ^{232}Th; 143 ± 11 Bq $kg^{-1}$for ^{238}U; and 200 ± 92 Bq $kg^{-1}$for ^{40}K. This observation is further confirmed by the calculated radiation hazard indices such as radium equivalent dose, external hazard index, representative gamma index, absorbed dose rate and annual effective dose. Therefore, the occupants in the area are at risk of high radiation exposure.

5.2 Recommendations

- This study should be extended to cover residential areas and indoor exposure. Plant and water samples should also be considered, whereby, all common food crops and water sources such as rivers and boreholes are investigated.

- The current study covered only the topsoil. It would therefore be important that further research be conducted in the lower soil profiles and rock samples.

- High radioactivity levels were recorded in this study, with radiation indices showing the public are at high risk. The radiation protection board should ensure protective measures are in place and the public are well informed of the hazardous effects of ionizing radiation.

References

Achola, S. O., Patel, J. P., Mustapha, A. O., and Angeyo H. K. (2012). Natural radioactivity and external dose in the high background radiation area of Lambwe East, Southwestern Kenya. *Radiation protection dosimetry*, 152(4): 423 - 428.

Ademola A. K., Bello A. K., and Adejumobi A. C. (2014). Determination of natural radioactivity and hazard in soil samples in and around gold mining area in Itagunmodi, south-western, Nigeria. *Journal of radiation research and applied sciences*, 7: 249 – 255.

Adepoju-Bello, A. and Alabi, O. (2009). Heavy metals: A review. *The Nigerian Journal of Pharmacy*, 37: 41 - 45.

Akan, J., Abdulrahman, F., Sodipo, O., Ochanya, A. and Askira, Y. (2010). Heavy metals in sediments from River Ngada, Maiduguri Metropolis, Borno State, Nigeria. *Journal of Environmental Chemistry and Ecotoxicology*, 2(9):131 - 140.

ANL, Argonne National Laboratory, (2005). *Human Health fact Sheet: Asian Transactions on Basic and Applied Sciences*. ATBAS ISSN: 2221-4291.

ATSDR (2004). *Toxicological profile for strontium*. Atlanta, GA, United States Department of Health and Human Services, Public Health Service, Agency for Toxic Substances and Disease Registry.

Bashir G., Mohammad S., Azhar A. and Farouk A. (2012). Determination of radioactive elements and heavy metals in sediments and soil from domestic water sources in northern peninsular Malaysia. *Environmental Monitory and Assessment*, 184: 5043 – 5049.

Beckhoff, B., Kanngierfer, B., Weddel, R., Wolff, H. and Langhoff, N. (2006). *Handbook of Practical X-Ray Fluorescence Analysis*, Springer, Berlin.

Chang, R. (2005). *Nuclear Chemistry*. New York: MC-Grill.

Darko, E. O., Tetteh, G. K. and Akaho E. H. (2005). Occupational Radiation Exposure to NORMS in Gold Mine, *Radiation Protection Dosimetry*, 114(4): 538 - 545.

Dill, H. G. (2010). The "chessboard" classification scheme of mineral deposits: Mineralogy and geology from aluminum to zirconium. *Earth Science Reviews*, 100: 401 – 420.

EPA, Environmental Protection Agency, (2012). *Ionizing radiation Fact book*. EPA Office of Radiation and Indoor Air. EPA-402-F-06e061.

Fodor, M., Hegedus, A. and Stefanovits-Banyai E. (2005). Zirconium induced physiological alterations in wheat seedlings. *Biol. Plantarum*, 49: 633 – 636.

Gilmore, G. & Hemingway, J. D. (1995). *Practical Gamma Spectrometry*, John Wiley and Sons, NY, NY.

IAEA (1989). *Construction and Use of Calibration Facilities for Radiometric Field Equipment*, IAEA Technical Report 309. Vienna, IAEA.

IAEA (2003), *Guidelines for radioelement mapping using gamma-ray spectrometry data*, IAEA report, Vienna, Austria.

ICRP (2007). *Recommendation of the international commission on radiological protection*, ICRP publication 103; ICRP 37 (2 - 4).

Kabata-Pendias A., (2001). Trace elements in soils and plants, 2nd edn. CRC, Boca Raton.

Karangwa E. (2012). *Spectroscopic analysis of tungsten mining associated heavy metals and radionuclides and evaluation of impact on agricultural soil in selected areas of Rwanda.* M.Sc. thesis, University on Nairobi.

KCG, Kwale County Government (2015). *Mining potential and activities.* Extrated on January 2015 from; http://www.kwalecountygov.com/index.php?option=com_content&view=featured&Itemid=937

Lipsztein, J. L., Dias da Cunha, K. M., Azeredo, A. M., Juliao, L., Santos, M., Melo, D. R. and Simeoes Filho, F. F. (2001). Exposure of workers in mineral processing industries in Brazil, *Journal of Environmental Radioactivity*, 54: 189 - 199.

Maina D. N., (2008). *Measurements of heavy metals and natural radioactivity levels in soils around the titanium mining site in kwale district*. M.Sc. thesis, University of Nairobi.

Maina, D. M., Kinyua A. M., Nderitu S. K., Agola J. O. and Mangala M. J. (2002). *Indoor Radon (222 Rn) Levels in Coastal and Rift Valley Regions of Kenya*. International Atomic Energy Agency (IAEA), IAEA-CN-91/56, 401 - 405.

Mohammed N. K. and Mazunga, M. S. (2013). Natural Radioactivity in Soil and Water from Likuyu Village in the Neighborhood of Mkuju Uranium Deposit, *International Journal of Analytical Chemistry* , Volume 2013, Article ID 501856,.

Mohanty, A. K., Sengupta, D., Das, S. K., Vijayan, V. and Saha, S. K. (2004). Natural radioactivity in the new discovered high background radiation area on the eastern coast of Orissa, Indi. *Radiation measurements, International congress series*, 1276(38): 153 - 165.

Mustapha A. O., Mbuzukongira P. and Mangala M. J. (2007). Occupational radiation exposures of artisans mining columbite-Tantalite in Eastern Democratic Republic of Congo. *Journal of Radiological Protection*, 27: 187 - 195.

Mustapha, A.O., Patel J.P. and Rathore I.V., (1997). Assessment of Human Exposures to Natural Sources of Radiation in Kenya. *Radiation protection dosimetry*24 (4) 387 - 396..

Muwanguzi J. B., Karasev V., Byaruhanga K., and Jönsson G. (2012). Characterization of chemical composition and microstructure of natural iron ore from Muko deposits. *ISRN, Materials Science,* http://dx.doi.org/10.5402/2012/174803

Nisar A., Mohamad S. J., Muhammad B. and Muhammad R. (2015). An overview on measurements of natural radioactivity in Malaysia. *Journal of Radiation research and applied sciences,* 8: 136 – 141.

Ntihabose L. (2010). *Assessment of Heavy Metal Fluxes and Radiation Exposure due to NORM in the Extraction and Processing of Coltan Ores in Selected Areas of Rwanda.* Extracted on January 2015 from; http://erepository.uonbi.ac.ke:8080/xmlui/handle/123456789/10991

Odumo, O. B., Mustapha, A. O., Patel, J. P., and Angeyo H. K. (2011). Radiological survey and assessment of associated activity concentration of the naturally occurring radioactive materials (NORM) in the Migori artisanal gold mining belt of southern Nyanza, Kenya. *Applied Radiation and Isotopes,* 69(6): 912 - 916.

Otwoma, D., Patel, J. P., Bartilol, S., Mustapha A. O., (2013). Estimation of annual effective dose and radiation hazards due to natural radionuclides in Mount Homa, southwestern Kenya. *Radiation protection dosimetry*, 155(4): 497 - 504.

Oyedele, J. A. (2006). Assessment of the natural radioactivity in the soils of Windhoek City, Namibia, Southern Africa. *Radiation Protection Dosimetry*, 121(3): 337 - 340.

Paschoa, A.S. (2000). More than forty years of studies of natural radioactivity in Brazil. *Technology*, 7:193 – 212.

Patel J. P. and Mangala M. J. (1994). Elemental analysis of carbonatite samples from Mrima Hill, Kenya, by energy dispersive X-ray fluorescence (EDXRF). *International journal of radiation applications and instrumentation,* 8(4): 389 - 393.

Patel, J. P. (1991). Environmental radiation survey of the area of high natural radioactivity of Mrima hill of Kenya. *Discovery and Innovation*, 3(3): 31 - 36.

Preston D. L., Shimizu Y., Pierce D. A., Suyama A., and Mabuchi K. (2003). Studies of motality of atomic bomb survivors.Report 13: solid cancer and non-cancerndisease mortality, 1950 – 1997. *Radiation resources*, 160: 381 – 407.

RPB, Radiation Protection Board, (1999). *Radioactivity Investigations at Mrima Hill murrum quarry and associated graveled roads in Kwale District.* Ministry of health, Kenya.

Sánchez-González S., Curto N., Caravantes P. and García-Sánchez A. (2014). Natural gamma radiation and uranium distribution in soils and waters in the Agueda River Basin (Spain-Portugal). *Procedia earth and planetary science*, 8: 93 – 97.

Sitko, R., and Zawisza, B. (2012). Quantification in X-Ray Fluorescence Spectrometry. INTECH Open Access Publisher.

Sivakumara, S., Chandrasekaran, A., Ravisankar, R., Ravikumar, S.M., Jebakumar, J. P., Vijayagopal, P., Vijayalakshmi, I., Jose, M.T. (2014). Measurement of natural radioactivity and evaluation of radiation hazards in coastal sediments of east coast of Tamilnadu using statistical approach. *Journal of Taibah University for Science*, 8: 375 – 384.

UNSCEAR, (1993). *Radiation exposure from natural sources of radiation*. New York: United Nation.

UNSCEAR, (2000). *Report on effects of atomic radiation to the general assembly*. New York: United Nations.

UNSCEAR, (2012). *Sources, effects and risks of ionizing radiation,* Report to the General Assembly, United Nations.

Van Grieken, R. and Markowicz, A. (2001). Handbook on X-ray spectrometry. CRC Press, New York.

Wei, L., Zha, Y., Tao, Z., Hew, C. and Yuan, H, (1993). Epidemiological investigation in high background radiation areas of Yangjiang, China, *Ramsar*, 3: 523 - 547.

WHO, 2010. Strontium and strontium compounds. Geneva : World Health Organization.

Wuana, R. and Okieimen, F. (2011). Heavy metals in contaminated soils: A review of sources, chemistry, risks and best available strategies for remediation. *International Scholarly Research Network ISRN Ecology*, 10: 5402 – 5424.

Yadav S. (2010). Heavy metals toxicity in plants: An overview on the role of glutathione and phytochelatins in heavy metal stress tolerance of plants. *South African Journal of Botany*, 76: 167 – 179.